

Article

Design Improvement Using Topology Optimization for the Structural Frame Design of a 40 Ft LNG ISO Container Tank

Tuswan Tuswan ^{1,*}, Muhammad Andrian ¹, Wilma Amiruddin ¹, Teguh Muttaqie ², Dian Purnama Sari ³, Ahmad Bisri ³, Yuniati Yuniati ³ , Meitha Soetarjo ³, Muhammad Ridwan Utina ³ and Rudias Harmadi ³

¹ Department of Naval Architecture, Universitas Diponegoro, Semarang 50275, Indonesia; muhammadandrian24@gmail.com (M.A.); wilmaamiruddin@lecturer.undip.ac.id (W.A.)

² Research Center for Testing Technology and Standards, National Research and Innovation Agency (BRIN), South Tangerang 15314, Indonesia; tegu019@brin.go.id

³ Research Center for Hydrodynamics Technology, National Research and Innovation Agency (BRIN), Surabaya 60117, Indonesia; dian.purnama.sari@brin.go.id (D.P.S.); abis001@brin.go.id (A.B.); yuni006@brin.go.id (Y.Y.); meithasoetardjo@gmail.com (M.S.); muha009@brin.go.id (M.R.U.); rudi003@brin.go.id (R.H.)

* Correspondence: tuswan@lecturer.undip.ac.id

Abstract: LNG ISO tank containers are a solution for bulk liquefied natural gas (LNG) delivery to the outer islands of Indonesia that are not connected to the gas pipeline network. The design of an ISO tank frame must consider two critical parameters, strength/rigidity and weight saving, which affect the operational performance of the distribution process. The current investigation aims to numerically optimize the design of the structural frame of a 40 ft LNG ISO tank for a mini LNG carrier operation using a topology optimization framework. Two design solutions are used in the topology optimization framework: reducing the strain energy and mass retained. Mass retained was selected as the objective function to be minimized, which was assumed to be 60–80%. The proposed frame design is tested using three operational loading scenarios, including racking, lifting, and stacking tests based on the ISO 1496 standard. The convergence mesh tests were initially evaluated to obtain the appropriate mesh density in the finite element analysis (FEA). The simulation findings show that the topology optimization method of the frame design resulted in an improved design, with an increase in the strength-to-weight saving ratio. A promising result from the optimization scenario demonstrates weight savings of about 18.4–37.3%, with experienced stress below the limit criteria. It is found that decreasing mass retained causes a significant stress increase in the structural frame and ISO corner castings, especially in the stacking load. The critical recommendation in the frame design of the LNG ISO tank can be improved by eliminating the saddle support and bottom frame and increasing the thickness of the vertical frame.

Keywords: 40 ft ISO tank; frame design; topology optimization; finite element analysis



Citation: Tuswan, T.; Andrian, M.; Amiruddin, W.; Muttaqie, T.; Sari, D.P.; Bisri, A.; Yuniati, Y.; Soetarjo, M.; Utina, M.R.; Harmadi, R. Design Improvement Using Topology Optimization for the Structural Frame Design of a 40 Ft LNG ISO Container Tank. *Designs* **2024**, *8*, 21. <https://doi.org/10.3390/designs8020021>

Academic Editor: Julian D. Booker

Received: 24 January 2024

Revised: 14 February 2024

Accepted: 19 February 2024

Published: 21 February 2024



Copyright: © 2024 by the authors. Licensee MDPI, Basel, Switzerland. This article is an open access article distributed under the terms and conditions of the Creative Commons Attribution (CC BY) license (<https://creativecommons.org/licenses/by/4.0/>).

1. Introduction

Liquified natural gas (LNG) is one of the alternative energy sources used to replace diesel fuel, which is in line with Indonesia's resources as one of the world's largest LNG exporters [1]. LNG is one of the strategic solutions for meeting the energy needs in Indonesia. In addition to using LNG as an alternative energy source, Indonesia needs to consider adequate distribution flow. Mini LNG carriers have become a widely convenient method for transporting liquefied natural gas (LNG) over both land and sea, maintaining its extremely cold temperature of -165°C [2]. The fact that mini LNG ISO tanks are now only available for import and that there are no set standards for ISO tank design at home is the reason behind Indonesia's interest in developing the technology of these tanks. Thus, a design study for LNG ISO tanks must be carried out to use the suggested process and guarantee structural safety and integrity.

LNG ISO tanks are containers used for transporting various gas products, liquids, and hazardous chemicals in large quantities safely and efficiently [3]. ISO tanks facilitate gas distribution to areas in Indonesia that still need to be connected to the gas pipeline network. In general, ISO tanks consist of an inner tank made of stainless steel, which can store liquids at -196°C , and an outer tank made of carbon steel as vacuum insulation to allow the insulation process to maintain the temperature of the cargo. The tank must be designed according to the standards of ASME Section VIII [4]. ISO tanks must have a solid structure, especially in the frame, to support and protect the tank and facilitate storage, securing, and handling according to ISO container standards [5].

The ISO tank frame design should consider several indicators, such as the safety and weight management of the design [6]. The frame must have an optimal stiffness value for increasing safety levels during shipping operations. The heavier the ISO tank frame, the more material directly used, which results in a greater compressive force on the ISO tank assembly. These two parameters also have an essential value in supporting the success of the ISO tank shipping process, which is mostly achieved by ship, affecting the transport ship's stability. Numerous studies applying type B and C LNG tanks [7–9] and apple-shaped tanks for LNG carriers [10] were carried out to assess the numerical analysis of structural assessment. In addition, the effect of liquid inertial force on stress distribution and safety level of the container tanks under various load conditions was examined using the FEA method [11,12]. Additionally, studies were performed on several pressure vessel head shapes, including conical, ellipsoidal, torispherical, flat, and hemispherical heads [13]. Although numerous studies were conducted, analytical studies on LNG ISO tank containers according to codes are limited. This arises from the difficulty of developing a reliable process for evaluating the structural integrity of ISO tank designs.

Design optimization is one method for developing an optimum design that optimizes weight and strength. Topology optimization has been successful in redesigning engineering products, especially marine structures. Islam et al. [14] discussed the topology weight optimization of the tanker transverse bulkhead structure using finite element-based software. The topology weight optimization of the very large crude carrier (VLCC) ship frame structure was carried out by Weiqiang et al. [15] using the finite element analysis approach. The investigation results conducted by Zhang et al. [16] discuss the topology optimization of the design weight of the pedestal structure on the ship using finite element-based software. Topology optimization methods can effectively produce rigid and lightweight designs for ship structural elements [17]. Pingale et al. [18] produced a lighter hull structure chassis design for wheeled combat vehicles using topology optimization. Topology optimization of lighter unmanned aircrafts was also successfully designed by Aribowo et al. [19]. Topology optimization successfully improved the strength of the fixed offshore structure design investigated by Hyun-Seok et al. [20]. Moreover, Deng et al. [21] investigated the optimal jack-up offshore platform leg structure design using the topology optimization method. Some of these studies have successfully used topology optimization to develop more optimal and efficient designs, significantly reducing the structural weight of a product without sacrificing the required structural strength.

Topology optimization is commonly utilized in engineering to create lightweight structural designs while preserving structural strength. Still, these studies have been limited and specifically applied to the frame design of the 40 ft LNG ISO tank model. To support the distribution of LNG in Indonesia, it is necessary to modify the structure of a lighter ISO tank frame using a proven topology optimization method. Based on the above-mentioned problem, the current study aims to propose an optimized ISO 40 ft LNG tank frame design using ABAQUS 6.20 version. The topology optimization method using the finite element analysis with ABAQUS 6.20 version will be used. Strain energy was selected as the objective function to be minimized, and the percentage of unused volume was assumed in the range of 60–80%, which was subjected to various operational loading conditions, such as stacking, lifting, and racking loading tests. The numerical validation was first conducted using mesh convergence analysis to obtain mesh efficiency with optimum computational time. The

result aims to obtain the optimum structural frame design by optimizing weight saving and structural performance in various operational conditions. This study may serve to minimize the cost of manufacturing LNG ISO containers by improving the structural frame design. A lighter and more efficient design may decrease material costs while preserving or increasing structural performance, providing economic benefits to manufacturers and end users. Manufacturers may match their products with the required safety and performance criteria by optimizing structural frame design, allowing it to fulfill regulatory standards and achieve commercial approval.

2. Materials and Methods

2.1. Topology Optimization Framework

Topology optimization in the FEA removes a certain amount of mass that is not needed by elements in the analysis either by reducing the element size or eliminating the number of elements to increase the layout efficiency, called the rejection ratio (*RR*). Elements with values far from the critical criteria or considered safe were eliminated or minimized, while the value of elements with the highest critical value was retained. The entire component only contained elements with critical values, so the mass was lighter but could withstand the critical loads [22]. This ensured that the resulting component was appropriately designed and efficient in material usage.

In this study, the topology optimization procedure of a 40 ft LNG ISO tank frame manufactured at National Research and Innovation Agency (BRIN), Surabaya, Indonesia consists of three main procedures. The first step is to validate the design conformity with the criteria according to ASME Section VIII standard [4] and evaluate the 40 ft LNG ISO tank truss structure through each loading scenario according to the ISO 1496 standard [23]. The goal is to determine the strength of the existing frame design to determine each component's strength.

In the general situation of topology optimization problems, an objective function called F is specified, and this function is subject to a volume constraint expressed as $G_0 \leq 0$. In addition, other constraints may be expressed as $G_i \leq 0$ for $i = 1, \dots, N$. The material distribution in the design domain Ω is described by a density $\rho(x)$, which has a value of 0 (indicating empty condition) or 1 (indicating the presence of solid material) at any point. Mathematically, this optimization problem can be formulated in Equation (1).

$$\begin{aligned} \min_{\rho} F &= \int_{\Omega} f(u(\rho), \rho) dV, \\ \text{subject to } G_0(\rho) &= \int_{\Omega} \rho(x) dV - V_0 \leq 0, \\ G_i(u(\rho), \rho) &\leq 0, \quad i = 1, \dots, M, \\ p(x) &= 0 \text{ or } 1, \quad \forall x \in \Omega, \end{aligned} \tag{1}$$

where the state domain u is linear or nonlinear equations, and the objective function in this context can be considered the integral of a local function $f(u(\rho), \rho)$ as an illustration. It can refer to the strain energy density when considering compliance optimization.

Two different methods can approximate Equation (1). The first approach is the Lagrangian approach, known as boundary following mesh, while the second formulation is the Eulerian approach using fixed mesh. In the Lagrangian method, generating more gaps in the optimal solution can be detrimental to the performance of the objective function. Meanwhile, in the Eulerian method, increasing some constraints may result in problems with similar gaps.

Another issue is related to the discrete nature of the density variable (0 or 1), which results in difficulty in finding the optimal solution. This constraint becomes especially significant in the context of the Eulerian method. To overcome this problem, an efficient

gradient-based optimization algorithm is required. The issue may thus also be seen as an optimization problem for continuous topology. Convergence within a reasonable number of iterations is guaranteed by these methods. We may state the problem using Equation (2) in this new framework.

$$\begin{aligned} \min_{\rho} F(u(\rho), \rho) &= \sum_j \int_{\Omega_j} f(u(\rho_j), \rho_j) dV, \\ \text{subject to } G_0(\rho) &= \sum_i v_j \rho_j - V_0 \leq 0 \\ G_i(u(\rho), \rho) &\leq 0, \quad i = 1, \dots, M, \\ 0 \leq \rho_j &\leq 1, \quad j = 1, \dots, N, \end{aligned} \tag{2}$$

where ρ refers to a vector of design variables with length N . In addition, the $f(u, \rho)$ component of Equation (2) describes the correlation between density and material properties, which can be formulated as $f(u, \rho) = 0$. In the formula, $g(\rho)$ is the density interpolation function, and $f_0(u)$ is the field function applicable to solid materials. The previously described approach is a method known as the approximate approach, where it is assumed that the equilibrium equations are satisfied at each stage of optimization.

In situations where structural constraints are met, the main goal of topology optimization is to reduce the strain energy in the structure. Adding stiffness to the structure will reduce this structural strain energy, which can be achieved by assigning density to individual element units through design variables. The strain energy (U) formulation can be expressed in Equation (3).

$$U = \frac{1}{2} V \sigma \epsilon \tag{3}$$

For instance, it is important to find the minimum statistical strain energy required for a given load in order to achieve maximum structural stiffness when calculating the highest static structural stiffness within volume constraints. This is essentially about determining the lowest compliance level. The second stage is the optimization process, which begins with determining the design region or the design to be optimized, as illustrated in Figure 1. The entire frame structure is selected as the design region at this stage. In the optimization process, it is also necessary to determine the design response. The design response is the strain energy. Strain energy was chosen as the objective function to be minimized, and the percentage of unused volume was 60–80%. The optimization process can be executed by selecting the limit option of 50 design cycles, because the topology optimization process generally reaches a convergence value of 25–40 cycles [19]. The optimization process was stopped until the minimum strain value was obtained. The final step is to redesign the optimization results. It is required to improve the geometry to make the design more realistic for the manufacturing process. The results of the redesign are carried out with ISO 1496 loading conditions to find the shortcomings in the design so that they can be corrected and an improved design proposed.

2.2. ISO Tank Design Requirement

2.2.1. Design Parameter of ISO Tank

The 40 ft LNG ISO tank is a common container for storing and transporting LNG. This tank plays a vital role in the global LNG supply chain as it was constructed using high-quality materials and designed to withstand various conditions. Figure 2 illustrates the geometry of the outer and inner shells of an ISO tank. This section addresses the proper material selection and determination of the required thickness for a 40 ft LNG ISO tank pressure vessel. ASME Sections II and VIII [4,23] were used as guidelines to determine material selection, allowable material stress limits, and pressure vessel thickness calculation methods.

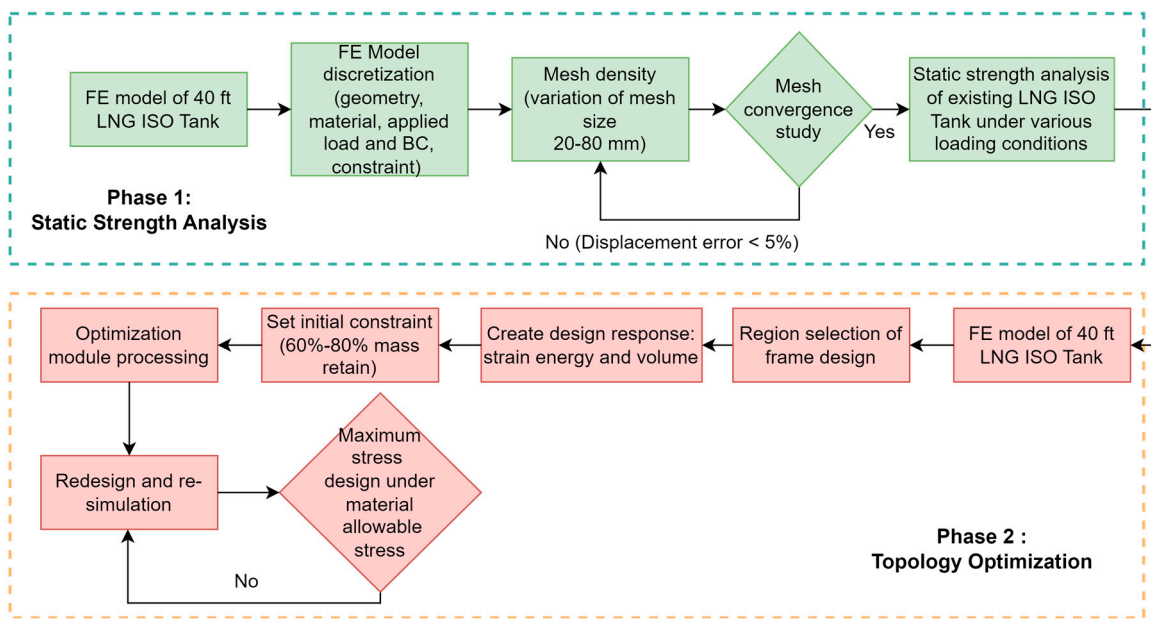


Figure 1. ISO tank topology optimization framework.

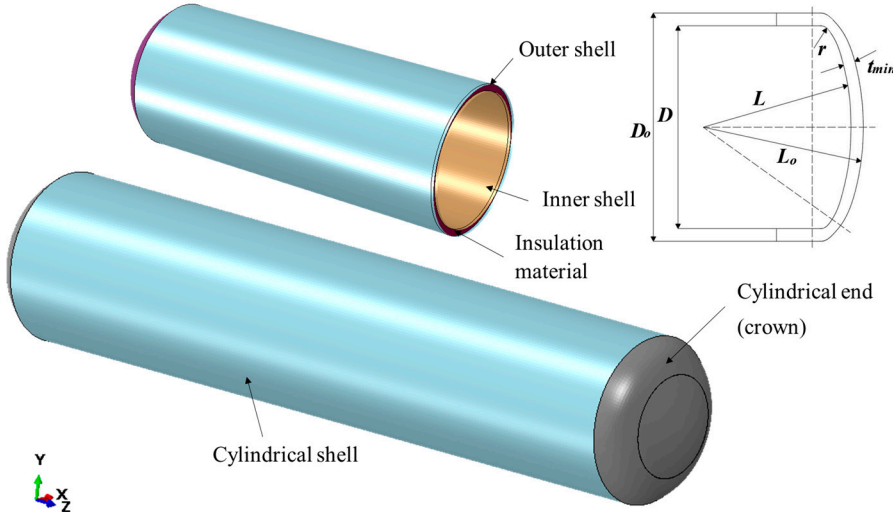


Figure 2. ISO tank cylindrical shell geometry.

The material selected for calculation was SUS 304L alloy steel manufactured Surya Logam Universal Tbk, Tangerang, Indonesia from Krakatau Steel, known in the ASME Section II specifications [24] as SA 240 Gr 304L-S 30403. The material is referred to as a grade 304L (low carbon) stainless steel material with the designation UNS S30403. ASME Section II [24] strictly regulates material properties and categorizes them by nominal material composition type. Following the strict ASME rules ensured that the material selection and pressure vessel thickness calculations complied with the safety and functionality standards required in LNG transportation. A methodical approach is crucial for guaranteeing the structural stability and operational reliability of LNG ISO tanks, while also minimizing potential hazards and ensuring the safe transportation of LNG. The calculation for minimum thickness is outlined in UG-27 of ASME VIII-1 [4], and the input parameters are detailed in Figure 2. According to the code, the thickness must exceed the predicted result, as determined by Equation (4).

$$t = \frac{PR}{SE - 0.6P} \quad (4)$$

where P is the internal design pressure, R is the inside radius, S is the allowable stress for stainless steel (SUS 304 L), and E is the butt joint efficiency. For more information, see the ASME Table UW-12 [4]. In addition, the calculation of the concave side of the toroidal shell for both ends of the cylinder, as shown in Equations (5) and (6), refers to Section UG-32.

$$t = \frac{PLM}{2SE + P(M - 0.2)} \quad (5)$$

$$M = 0.25(3 + \sqrt{\frac{L}{R}}) \quad (6)$$

where R is the inner radius in mm, and L is the inner crown radius in mm. Figure 2 provides a schematic geometrical description of the torispherical cylindrical shell.

Meanwhile, paragraph UG-28 Part VIII [4] calculates the maximum allowable external pressure for the cylindrical shell. In the first step, the geometry $D_0/t \geq 10$ must be verified. After the verification stage, the external load graph obtained from Figure G in ASME Section II, Part D, Subpart 3 [24], obtains the A value using the base values of L/D_0 and D_0/t . After obtaining the A value, the B value in Figure HA-3, which corresponds to the 304L material specification, is determined. Finally, the maximum value is obtained using the B value according to Equation (7). This procedure is similar to determining the convex side of the maximum cylinder end pressure based on UG-33. The B value is used in Equation (8).

$$Pa = \frac{4B}{3\left(\frac{D}{t}\right)} \quad (7)$$

$$Pa = \frac{B}{\left(\frac{R}{t}\right)} \quad (8)$$

This computation involves paragraph UG-29 of ASME Section VIII [4], used to determine the stresses in ring stiffeners within pressure vessels. The engineering process for this stage assumes the original dimensions and form of the stiffener ring.

$$B = 0.75\left(\frac{PD}{t + \frac{A_s}{L_s}}\right)/14 \quad (9)$$

where A_s is the expected cross-sectional area of the ring stiffener, L_s is the distance between the stiffeners, and t is the shell thickness predicted from the previous step. Next, the value of B is calculated using Equation (9). The B value can be used to find a value of A equal to the B value calculated using the external pressure table in ASME Section II, Part D [24].

$$I_{s'} = \left[D_0^2 L_s \left(t + \frac{A_s}{L_s}\right) A\right]/14 \quad (10)$$

$$I = \frac{twh_{wx}^3}{12} \quad (11)$$

The required moment of inertia for the ring stiffener is calculated using Equation (10). Finally, the true moment of inertia of the ring stiffener is ascertained, considering the initial assumptions laid out in Equation (11). Also, the required moment of inertia should be equal to or greater than the actual moment of inertia. The pressure vessel thickness results according to ASME Section VIII [4] are given in Table 1.

Table 1. The calculation result of pressure vessel thickness according to ASME Section VIII [4].

Parameter	Value (Unit)
Pressure of internal design (P_{int})	1 Mpa
Pressure of external design (P_{ext})	0.8 Mpa
Cylindrical length of inner tank (L_{cyl})	11,018 mm
Radius of inner crown (L)	2218 mm
Radius of inner knuckle corner (r)	221.8 mm
Thickness of inner shell (t)	7.1 mm
Thickness of inner head (t)	11.22 mm
Inner tank diameter (D)	2218 mm
Cylindrical length of outer tank (L_{cyl})	11,018 mm
Radius of outer crown (L)	1950.4 mm
Radius of outer knuckle corner (r)	243.8 mm
Thickness of outer shell (t)	3.95 mm
Thickness of outer head (t)	6.28 mm
Outer tank diameter (D)	2438 mm

2.2.2. ISO Tank Loading Parameter

The FEM analysis used ISO 1496 scenarios as the basis for strength calculations. To obtain certification and approval, new or modified designs had to pass the test according to the ISO 1496 standard [23]. The loading scenarios were calculated based on the ISO 1496 standard in Table 2. Based on the data, the 40 ft ISO tank was a Class A, which requires a stacking load of 942 kN at each leg/angle attachment point. Assuming a 40 ft ISO tank container with a gross weight of 32 tons, evenly distributed at each corner, results in a minimum load of 8 tons (73 kN). Thus, ISO 1496 specifies high-strength requirements estimated to withstand up to 3 levels (excluding the dynamic safety factor of 1.8). The ISO tank design layout is shown in Figure 3. A summary of the load layout scenarios is shown in Table 2.

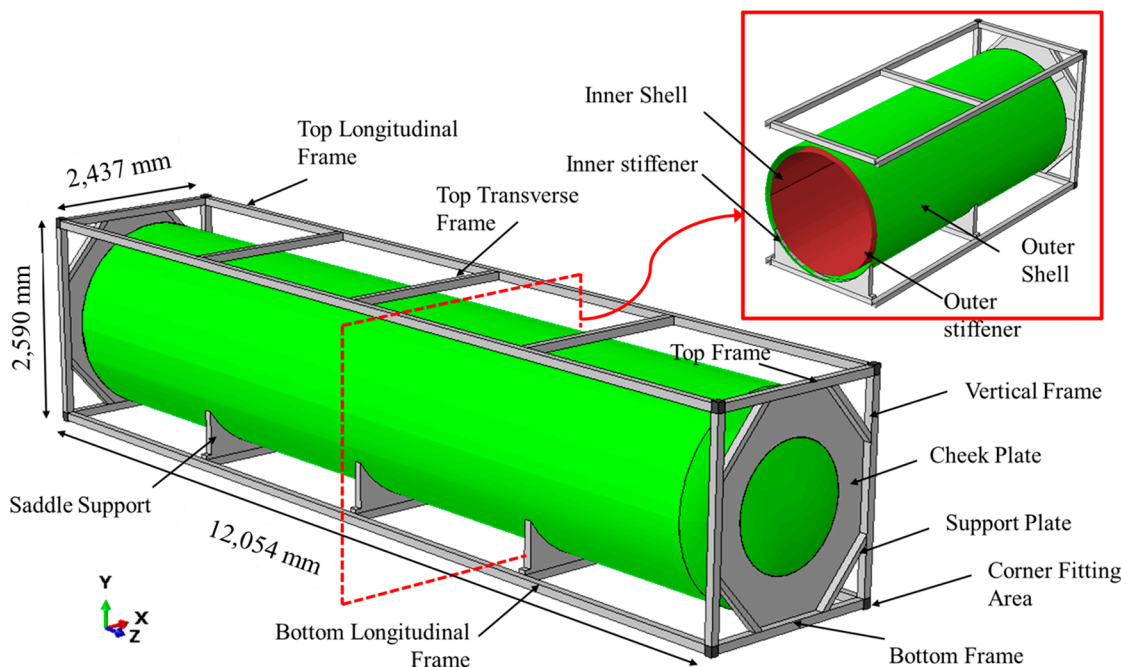
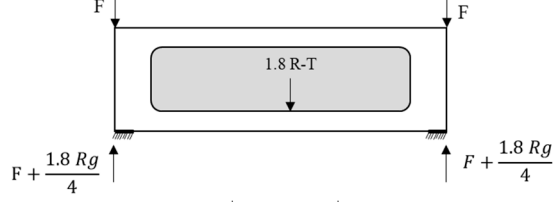
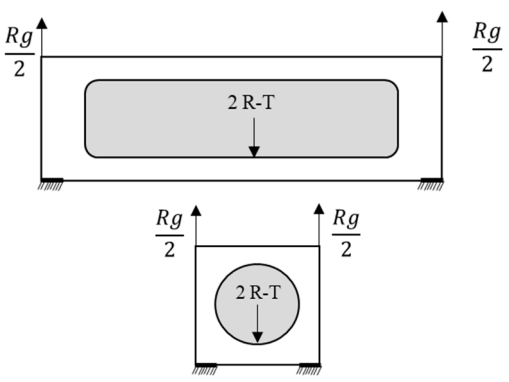
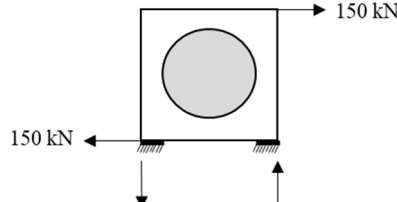
**Figure 3.** Design of 40 ft LNG ISO tank.

Table 2. Systematic loading conditions and layouts.

Load Scheme	Load Description	Loading Configuration
Stacking strength test	$F = 942 \text{ kN}$ $1.8 R - T = 444 \text{ kN}$ $942 + (\frac{1.8 Rg}{4}) = 1085 \text{ kN}$	
Lifting strength test	$\frac{Rg}{2} = 159 \text{ kN}$ $2R - T = 127 \text{ kN}$	
Racking (transverse) test	$F = 150 \text{ kN}$	

The loading scenario consists of three types, according to ISO 1496, listed in Table 2: stacking, racking, and lifting. To determine the amount of loading in each scenario, a model weight calculation must be performed in the software. The software calculated the total weight of the material and the thickness used in each part. The model's weight was obtained: tare weight (T) of 13.18 tons and gross weight (R) of 32.48 tons.

The stacking test was conducted to test the weight capacity of the 40 ft container to withstand the stacking load. Based on the ISO 1496 standard, the container was tested with a vertical load of approximately 942 kN (about 384 tons) applied simultaneously to all four corner joints or each pair of end joints. In addition, the LNG tank capacity contributed a displacement load of approximately 189.3 kN or 19.3 tons of cargo. This test was conducted to ensure the ISO tank structure could withstand the stack load at sea.

Lifting tests were also conducted to test the container's ability to withstand vertical lifting from four corresponding corner fittings. This test aimed to ensure the container floor's ability to withstand acceleration during crane handling. The test load should be evenly distributed on the floor so that the total weight of the container and the test load are $2R$. The container was lifted at the top four corners to avoid significant acceleration or deceleration forces. The gross (R) and tare (T) components were used in this test.

Lastly, a racking test was conducted to ensure the container's structural integrity when subjected to racking loads during transit via various intermodal modes such as ship and rail. In this test, the container tanks were supposed to be empty and loaded with 150 kN. The racking test was designed to evaluate the container's ability to withstand transverse racking forces on the end frames generated by ship motion.

2.3. Finite Element Analysis (FEA) Setup

2.3.1. Computational Domain and Material Selection

Finite element analysis (FEA) is a numerical simulation approach used in various engineering designs to investigate the behavior of structural and mechanical components [25]. ABAQUS/Standard 6.14 version was chosen as the FEA tool for modeling and simulation. The procedure consists of three stages: (1) SolidWorks created the ISO tank 3D model, (2) in the model discretization, geometry, material types, loading scenarios, and constraints were set for the model using ABAQUS, and (3) nonlinear static analysis was used to investigate the physical effects of these parameters.

The ISO tank geometry consists of several components: inner and outer shell, perforated baffle, ring stiffener, and structural frame. All of these components were accurately modeled to represent the actual tank dimensions. The tank material model was assumed to have linear elastic behavior transitioning to perfect plasticity. This theory assumes that the material behaves elastically up to a certain point, beyond which it undergoes plastic deformation with no further increase in stress. This means that the stress remains constant, while the material undergoes plastic deformation. The theory assumes ideal conditions such as uniform stress distribution and isotropic material properties. An elastic perfectly plastic material is widely used in engineering for its simplicity and ability to provide conservative estimates of material behavior under certain conditions. Material selection was made according to ASME Section II [24]. The material properties of LNG ISO tanks are wholly shown in Table 3. In this scenario, SA240Gr304L-PV material was used for the inner tank. Moreover, ASTM A516 carbon steel was used for the ring stiffeners, the outer tank, and the structural frame, including the saddle supports which used a steel frame.

Table 3. Material constants applied for LNG ISO tank.

Materials	Density	Young Modulus	Poisson's Ratio	Yield Strength
	ton/mm ³	MPa	-	MPa
Steel frame [26]	7.85×10^{-9}	210,000	0.3	340
SA240Gr304L-PV [24]	7.85×10^{-9}	193,000	0.3	175
ISO corner casting [23]	7.85×10^{-9}	215,800	0.3	275
Carbon steel ASTM A516 [27]	7.75×10^{-9}	200,000	0.3	248

2.3.2. Applied Boundary Condition and Contact Interaction

Kinematic coupling was performed with motion restraints in the upper and lower domains to reduce the computation time. This method used constraints to observe the motion of a rigid body from a specified reference point over a set of nodes. Within the group, the connected nodes were effectively locked together. Because kinematic coupling restrictions permitted the connection of continuum and structural elements, they were highly useful in load application scenarios. This made sure that the various components of the model worked together cohesively, which made proper load distribution easier. The boundary constraints applied to the ISO tank model are depicted in Figure 4.

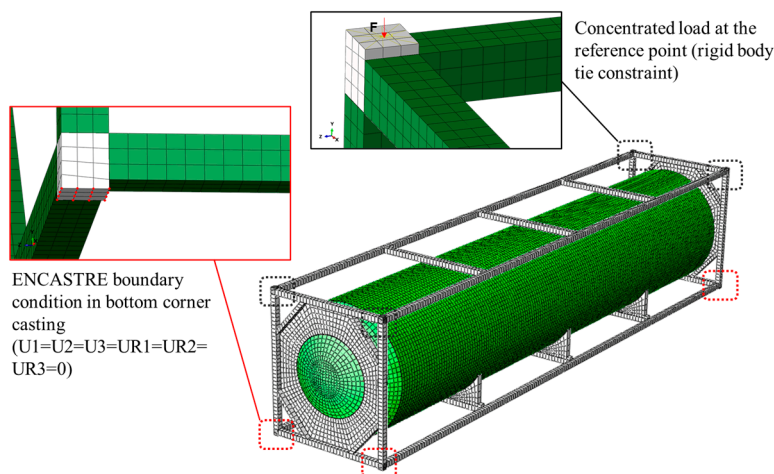


Figure 4. A fixed boundary condition was implemented at the bottom corner, while a concentrated load scheme was applied at the top corner.

In this current model, the tie constraint interaction was applied to the tank model, which was in direct contact with the frame model. The function of the tie constraint interaction is to bind the points on the surface of the meeting parts. Figure 5 shows a visualization of this arrangement, which consists of two distinct areas. The first area involves the connection of the front and rear spherical tanks by using support plates on the rear and front structures through node-to-node ties. The tie constraint ensures a robust and reliable connection between these components, allowing them to interact effectively under various conditions. Meanwhile, a tie connects the lower cylinder tank to the saddle in the second area through a surface-to-surface tie constraint. With these restraints in place, a strong and consistent interaction between the tank and saddle could be ensured, allowing for proper load transfer.

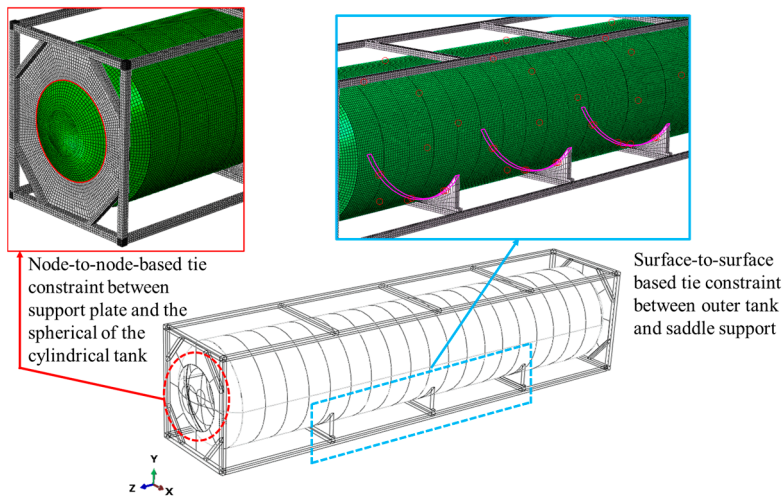


Figure 5. Constraint definition between support plate and cylindrical tank (red) and between outer tank and saddle support (blue).

2.3.3. Mesh Convergence Test

The convergence analysis was utilized to ascertain the optimal mesh size for computational efficiency [28]. Mesh refinement was achieved through either decreasing mesh size or augmenting node density within the mesh. The iterative process was undertaken until convergence was attained, necessitating a few adjustments for further mesh refinement. This investigation is primarily concerned with analyzing the displacement response of the structure to determine the most suitable mesh size across various loading conditions.

Finite element (FE) simulations were conducted with tetrahedral mesh sizes in the range of 40–80 mm, as depicted in Figure 6. Specifically, a structural frame and pressure vessel employed a four-node, quadrilateral stress/displacement shell element with reduced integration elements (S4R), while ISO corner casting utilized eight-node linear brick reduced integration hourglass control solid elements (C3D8R), offering a solution of comparable accuracy at reduced computational expense. Convergence was achieved using a mesh size of 50 mm, comprising a total of 74,800 elements, as depicted in Figure 7.

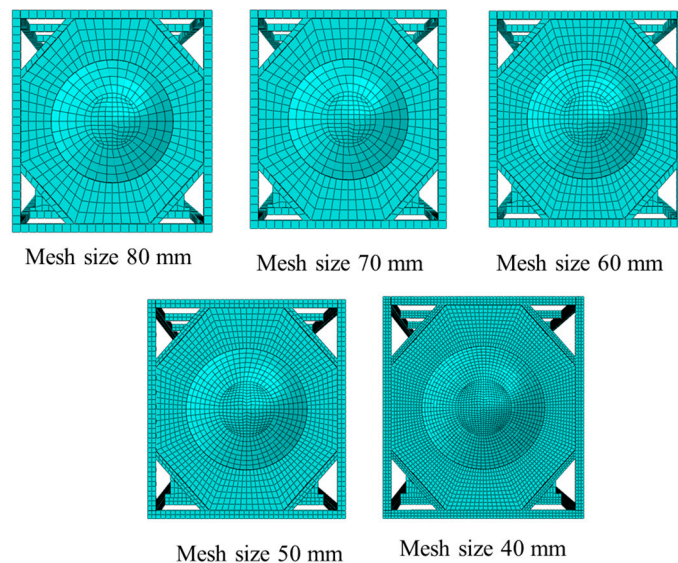


Figure 6. Various mesh size layouts on frame and tank structure.

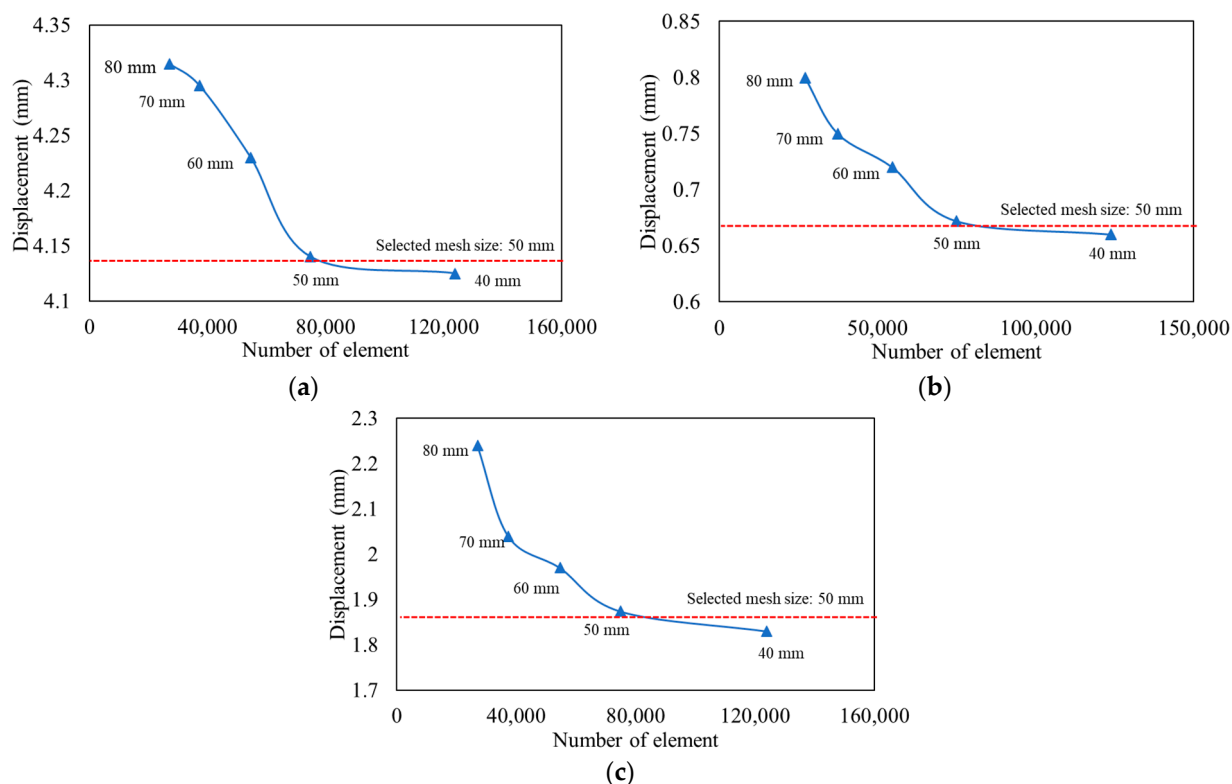


Figure 7. Convergence assessment under different loading tests: (a) stacking load scenario, (b) lifting load scenario, and (c) racking load scenario.

2.3.4. Design Variable

An LNG tank container comprises two basic structures: the pressure vessel and the structural frame. The structural frame consists of the tank mountings/corner fittings, end structure, and saddle supports, which transmit forces from the lifting and handling operations. The pressure vessel consists of the inner shell, insulation panel, baffle, outer shell, and ring stiffener. Data regarding the reference model are sourced from a prior study developed by the National Research and Innovation Agency (BRIN), Surabaya, Indonesia [29]. The current study aimed to find the most efficient tank frame design using topology optimization. Optimization was performed on the structural frame to eliminate elements that were far from critical stress without compromising the integrity of the structural strength. The part of the frame selected as the optimization region is shown in Figure 8. The optimization region is highlighted in the blue area, including the frame, check plate, and saddle support. The redesign was also determined by simulating predetermined loads, including stacking, lifting, and racking.

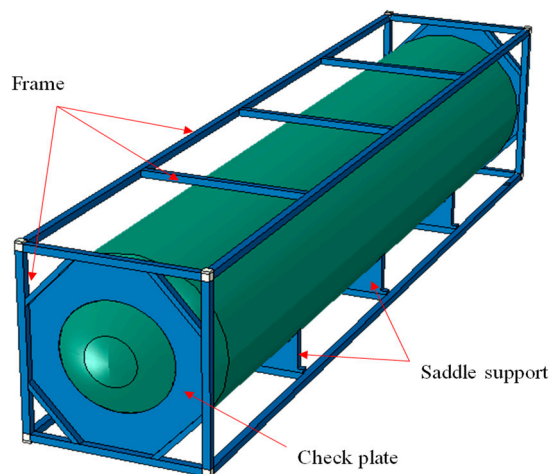


Figure 8. Optimization region on the structural frame of ISO tank model.

3. Results and Discussion

3.1. Result of Initial LNG ISO Tank Design

The simulation used three loading scenarios: racking, lifting, and stacking strength tests. The simulation result was divided into three main parts: the frame, pressure vessel, and ISO corner casting. Figure 9 illustrates the maximum stress values in each load scenario. It can be seen that among the structural parts and the load simulation scenarios, the structural frame experienced the highest stress level compared to the pressure vessel and ISO corner casting because the structural frame served to support the weight of the tank and cargo. However, the stress was still below the allowable stress (yield strength) of the steel material at 340 MPa. It was inversely proportional to the stress experienced by the pressure vessel, which had the lowest stress level because the pressure vessel design was specifically designed to withstand the internal forces exerted by the cargo, thus ensuring its containment without compromising the tank's structural integrity.

Furthermore, it can be observed that stacking was a critical load condition when compared to other loading scenarios. The LNG ISO tank seemed to have an excessive stacking load because in real operations, ISO tanks are treated differently than ordinary solid goods containers and can only be stacked up to two tiers. Similar results were found in previous studies [5,29], demonstrating that stacking and longitudinal racking loads are the critical loads in LNG operation.

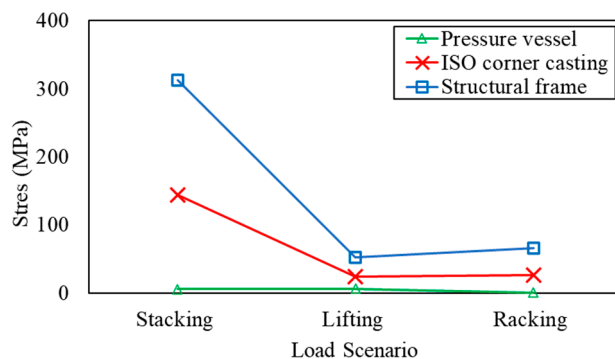


Figure 9. Comparison of maximum stress values of the ISO tank on each load scenario.

Figure 10 explains the maximum structural frame stress contours in each loading scenario. The highest stress occurred in the stacking loading scenario, which was 313.865 MPa, which occurred in the vertical frame. Overall, the maximum stress point occurred in the vertical frame because this part interacted directly with the ISO corner casting, which was the center of the load. It can be seen that the vertical frame became a critical location compared to the longitudinal frame, transverse frame, and saddle support.

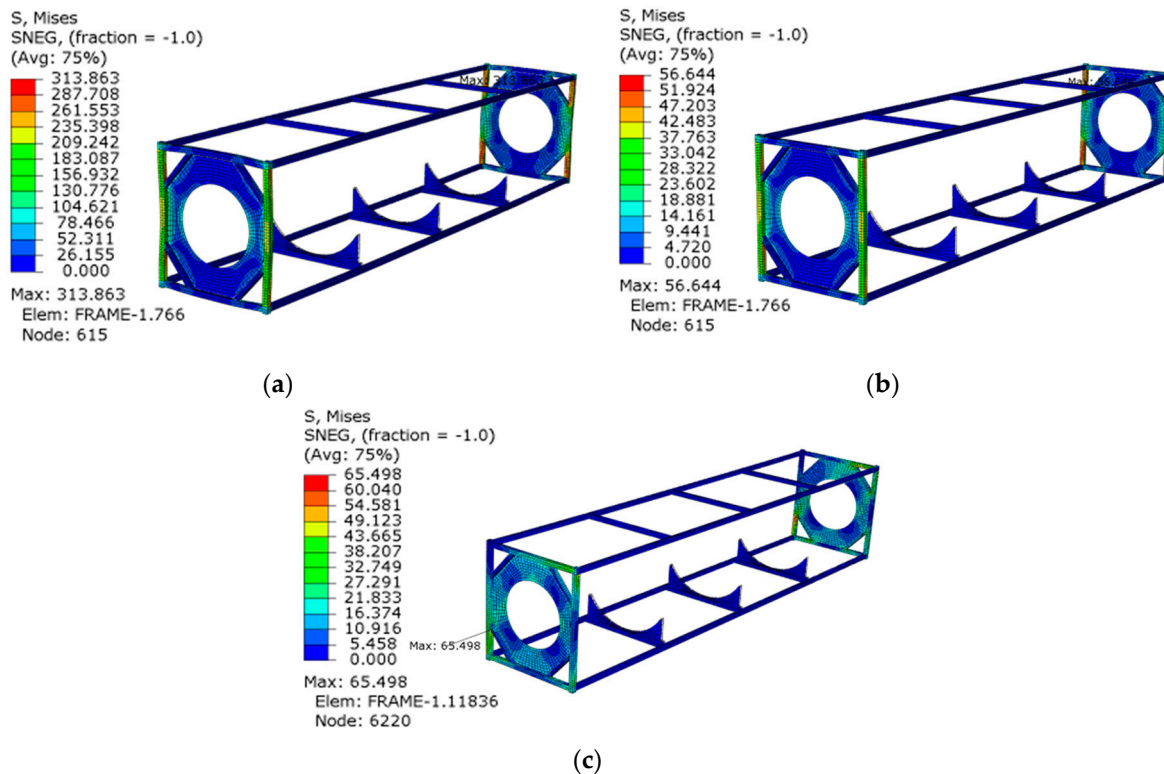


Figure 10. Comparison of ISO tank model stress contours: (a) stacking load scenario, (b) lifting load scenario, and (c) racking load scenario.

Figure 11 explains the displacement value of the LNG ISO tank model against different loading variations. The structural frame and ISO corner castings experienced higher displacement compared to the pressure vessel. A similar result was found: the critical load was a stacking test with the highest experienced displacement. Figure 12 describes the displacement contour of the structural frame in three different loading scenarios. It can be found that the highest displacement occurs at corner casting due to the stacking load scenario at 2.535 mm. In the stacking and lifting load scenarios, the maximum displacement occurred at the ISO corner casting section because this section was the center

of the downward load direction. In the racking load scenario, the longitudinal frame experienced the maximum displacement because of the direction of the transverse racking force on the end frames, so the longitudinal frame had the critical structure to maintain structural integrity.

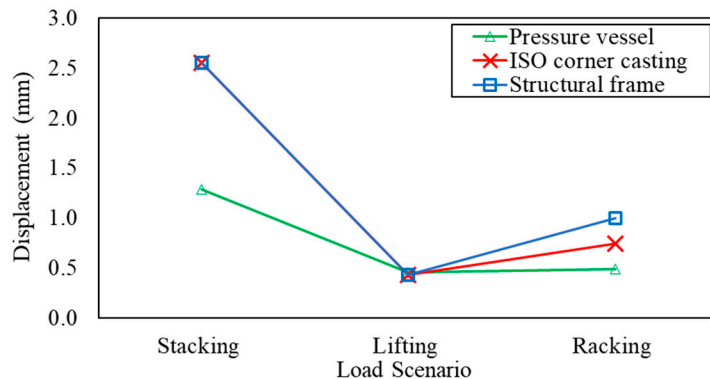


Figure 11. Comparison of maximum displacement values of the iso tank on each load scenario.

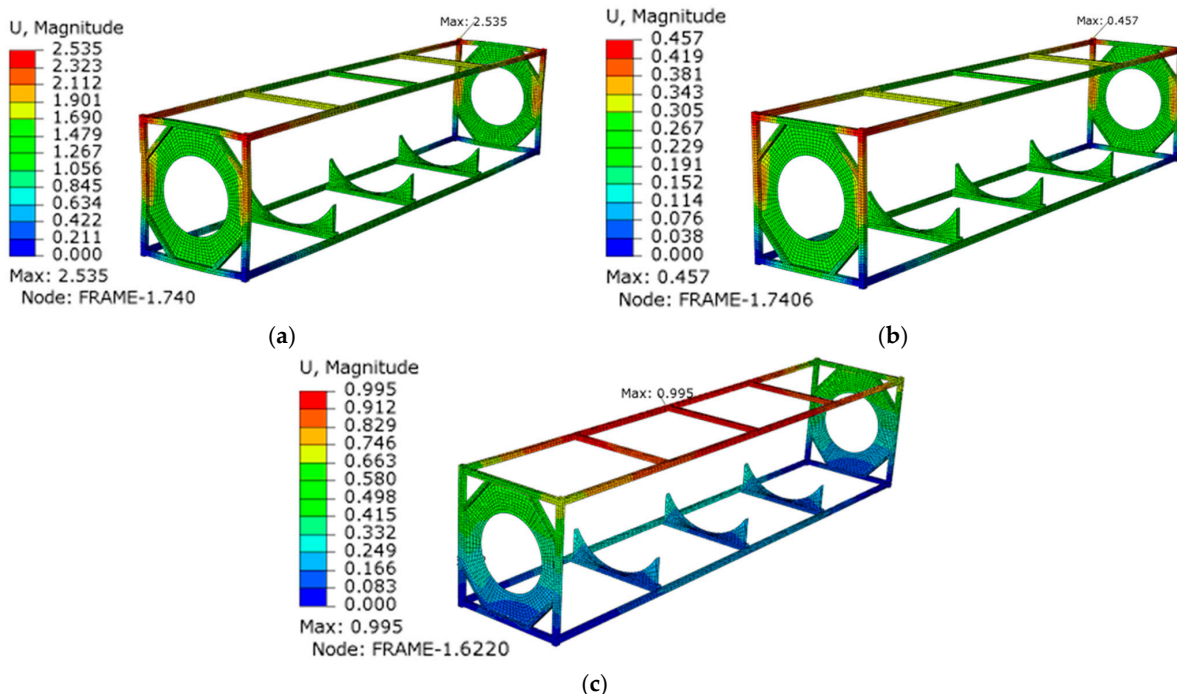


Figure 12. Comparison of ISO tank model displacement contours: (a) stacking load scenario, (b) lifting load scenario, and (c) racking load scenario.

Figure 13 compares the safety factor values for each structural part of the ISO tank model. The permissible stress of the structural frame, pressure vessel, and ISO corner casting are 340, 175, and 275 MPa, respectively. The safety factor is a parameter quantifying the degree of safety inherent in the structural strength, delineating the extent to which the structure can tolerate loads exceeding the predetermined design thresholds without compromising its integrity. The ratio of yield stress and maximum stress is defined as the safety factor. The analysis result showed that the safety factor values due to different loading conditions are all above 1, indicating the experienced stress is below the design limit. It can be found that the lowest safety factor value was experienced in the structural frame under stacking load. However, the value found is still safe to withstand the given load. In contrast, the highest safety factor value was found in the pressure vessel in the racking load, so the load carried in the tank can be guaranteed as safe.

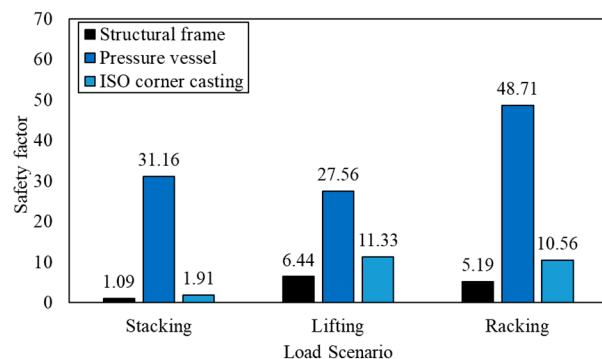


Figure 13. Comparison of safety factor values of ISO tank design models.

3.2. Result of Topology Optimization of LNG ISO Tank Design

In this subsection, the result of topology optimization is presented. Based on the simulation results, the structural frame had the highest stress level, but it was still below the allowable stress of the material. The analysis showed that the vertical frame was the critical location with higher experienced stress, so the optimization region can be focused on the longitudinal frame, transverse frame, and saddle support, which have the lowest stress. This part of the structural frame was the part to be optimized, commonly called the optimization region in ABAQUS software. The mass retained in this topology optimization was determined in the 60–80% range, and then the strain energy was plotted for each simulation. Figure 14 shows the strain energy of different masses retained under three loading scenarios. It can be seen that 19 to 42 iterations were required to meet the convergence criteria in different loading scenarios.

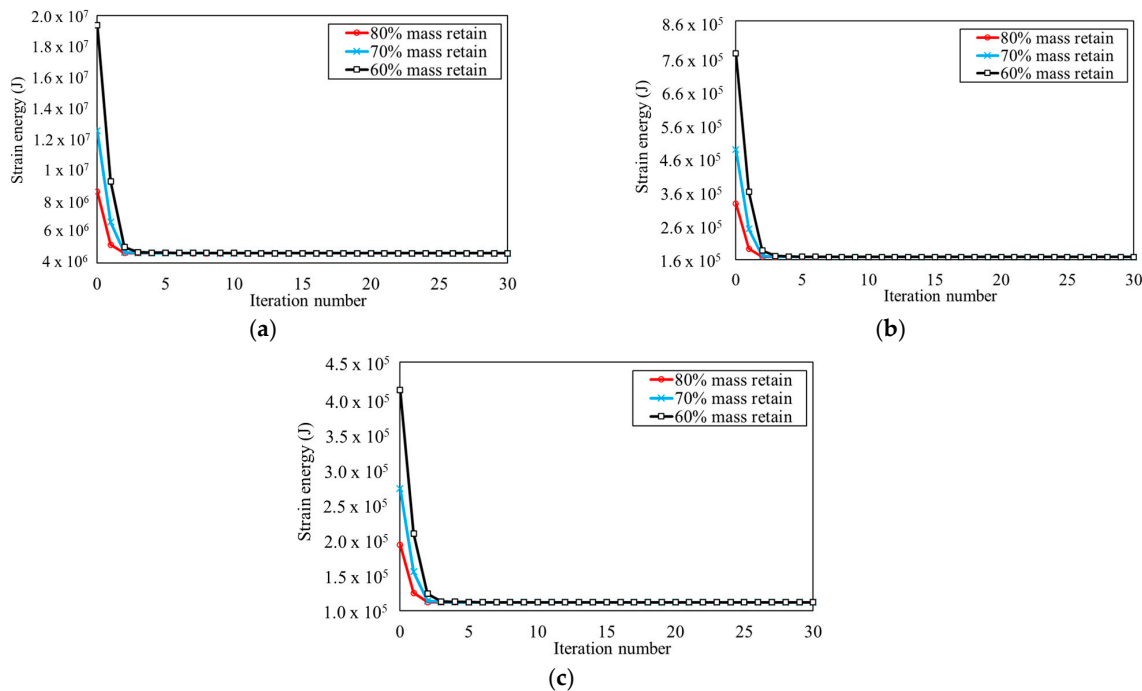


Figure 14. The comparison of strain energy between various masses retained: (a) stacking load scenario, (b) lifting load scenario, and (c) racking load scenario.

Figure 15 shows the optimization result of each mass retained, displaying three optimization results of a structural frame design that had slight differences, with some geometry parts being rough or disconnected. Redesigning the model's geometry was necessary to modify the design and improve the geometry. The results of this redesign process are shown in Figure 16. It can be found that several parts of the frame design, especially in the

bottom part, including the longitudinal frame, transverse frame, and saddle support, were eliminated and modified compared to the initial model.

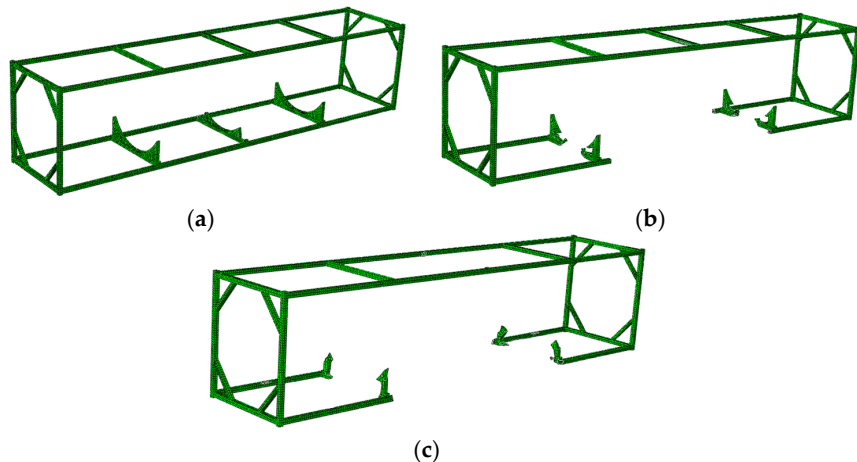


Figure 15. Optimization results of each mass retained: (a) 80%, (b) 70%, and (c) 60%.

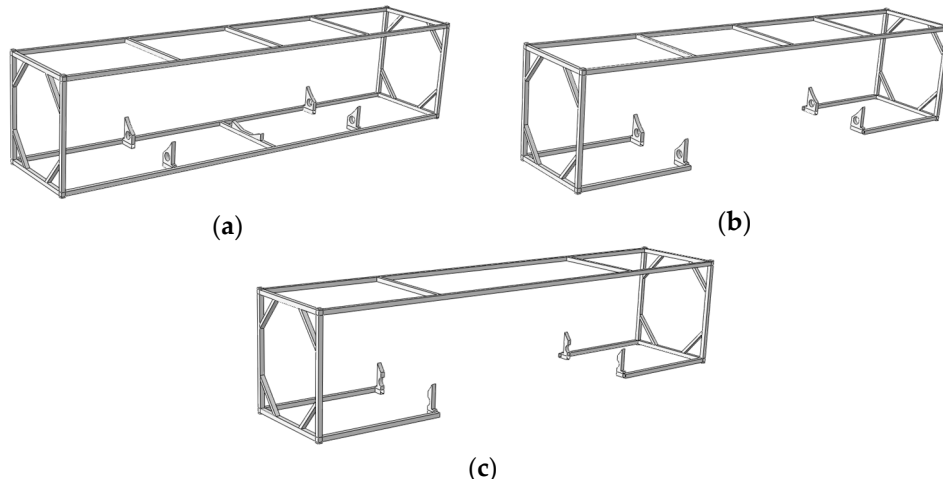


Figure 16. Redesigned frame optimization result of each retained mass topology: (a) 80%, (b) 70%, and (c) 60%.

3.3. Structural Performance of Optimized Design

Simulation of the optimized model must be performed to determine the maximum stress and displacement in the optimized model, which will be a consideration in determining the structural performance due to topology optimization. The simulation results are shown in Table 4, which compares the simulation results of the redesigned model in terms of maximum stress and displacement of the structural frame, pressure vessel, and ISO corner casting in each loading variation and mass retained.

Figure 17 shows that the decreasing mass retained causes a significant stress increase in the structural frame and ISO corner castings. It can be seen that the maximum stress value of the redesigned model showed a significant stress increase except in the pressure vessel. Comparing the changes in all evaluated loads, the maximum stress value increased in the stacking, lifting, and racking loading simulations on the structural frame and ISO corner casting. At the same time, the pressure vessel decreased in the stacking and racking simulation, and there was no change in the racking simulation. The most significant increase in the maximum stress value of the structural frame was experienced in the stacking loading scenario, falling within the range from 18.09 to 18.35%. Similarly, the ISO corner casting exhibited the most substantial rise in stress value under this loading condition, ranging from 38 to 38.3%. In contrast to the stress values observed in the pressure vessel section,

there was a slight stress reduction, specifically in the racking loading scenario, within the range from 30.7 to 31.03%.

Table 4. Von Mises stress and displacement of redesigned frame model in different load scenarios.

Load Scenarios	Mass Retained (%)	Von Mises Stress (MPa)			Displacement (mm)		
		Structural Frame	Pressure Vessel	ISO Corner Casting	Structural Frame	Pressure Vessel	ISO Corner Casting
Stacking	80	368.80	5.58	198.45	2.58	1.34	2.65
	70	368.81	5.54	198.65	2.58	1.34	2.65
	60	369.59	5.51	198.89	2.57	1.34	2.65
Lifting	80	61.86	6.30	33.28	0.43	0.45	0.45
	70	60.69	6.24	32.69	0.42	0.45	0.44
	60	60.42	6.21	32.51	0.42	0.45	0.43
Racking	80	75.66	0.41	34.08	0.98	0.49	0.74
	70	75.67	0.41	34.09	0.98	0.49	0.74
	60	76.16	0.41	34.17	1.00	0.49	0.74

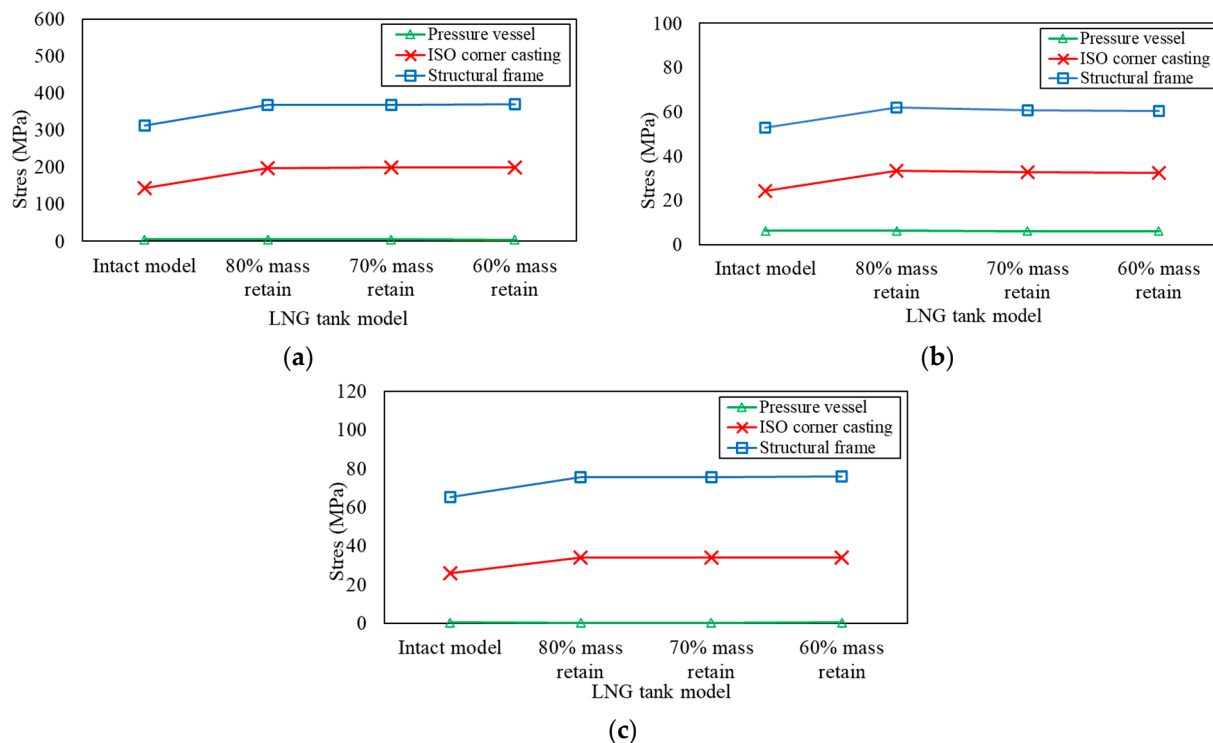


Figure 17. Comparison of maximum stress value of intact model with redesigned model: (a) stacking load scenario, (b) lifting load scenario, and (c) racking load scenario.

A comparison of displacement values for various redesign models in each loading scenario is shown in Figure 18. The outcome indicates that the structural frame and ISO corner casting endured the most significant displacement under stacking and racking loads. Moreover, the highest displacement can be found in the pressure vessel under the lifting load. It can be found that displacement values experienced a slight increase due to decreasing mass retained. The most significant increase occurred in the stacking loading scenario within the pressure vessel, falling within the range of up to 4.3%. It appeared because the applied force on the load was directly proportional to the weight generated on the model.

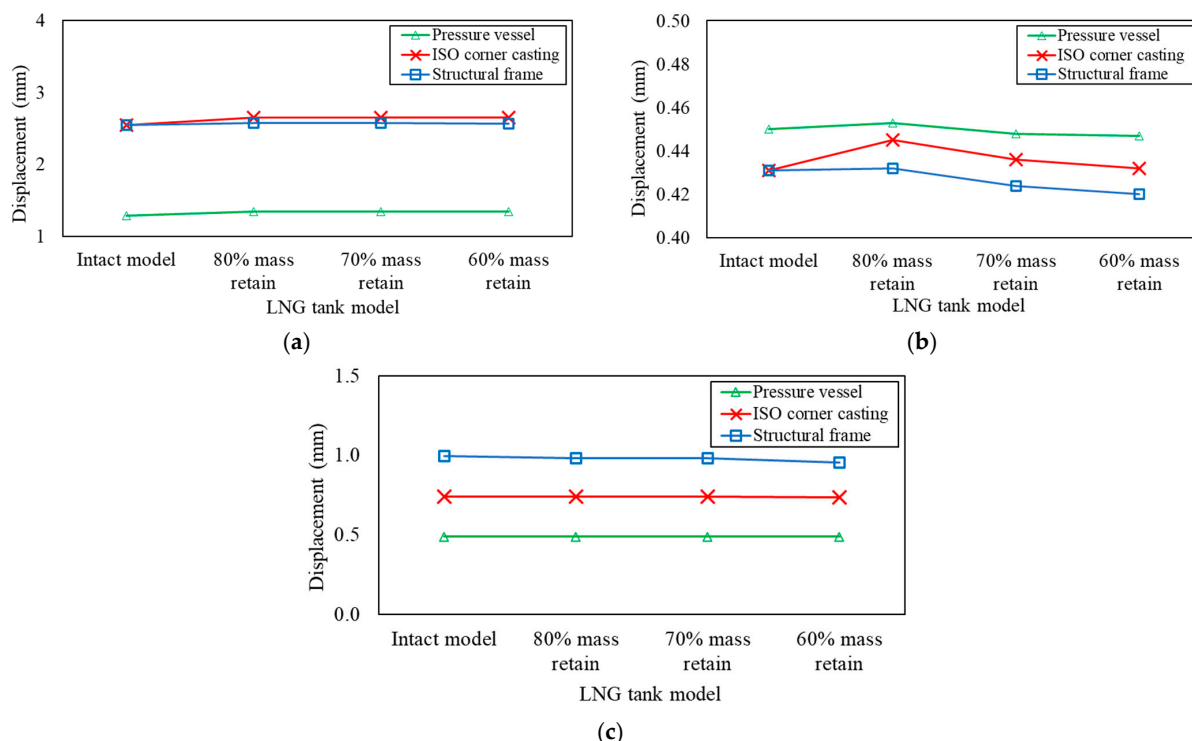


Figure 18. Comparison of maximum displacement value of intact model with redesigned model: (a) stacking load scenario, (b) lifting load scenario, and (c) racking load scenario.

Figure 19 shows the stress contour of the optimized model in the stacking load scenario under three different levels of mass retained. In the 60–80% mass retained model, it was found that the maximum stress occurred in the structural frame. The maximum stress on the structural frame of the 60, 70, and 80% retained model was located at the vertical frame, which had a stress value above the material's allowable stress of 340 MPa, which was 369.59 MPa, 368.81 MPa, and 368.80 MPa, respectively. It can be found that decreasing the amount of mass retained caused an increase in the maximum stress. It was caused by the removal of elements in the structural frame of this model, which was the most compared to other models, so the integrity of the structural frame was also reduced. Consistent with this stacking load scenario, it focused on applying downward pressure at each corner, which required the vertical frame plate to be thick enough to withstand it.

Figure 20 shows the displacement contour of the optimized model in the stacking load scenario under three different levels of mass retained. The maximum displacement value of the 60–80% retained model occurred at the ISO corner casting during the stacking load scenario because the ISO corner casting became the center point of loading. The maximum displacement value of the three optimized models did not change significantly, in the 2.645–2.652 mm range. This demonstrates that the topology optimization process did not influence the displacement value of LNG ISO tank models.

Figure 21 shows the comparison of mass between the intact model and redesigned models. The mass retained was the mass left on the model to be optimized, so the amount of mass retained significantly affected the model's weight that resulted from the topology optimization process. The smaller the mass retained, the more mass removed from the model. As evidenced in Figure 21, the weight reduction in the redesigned model was 18.4%, which occurred with 80% mass retained. Moreover, with 70% mass retained, there was a weight reduction of 31.4%, and with 60% mass retained, the weight reduction reached 37.3%. However, in the optimization results, the mass reduction in the model was not in accordance with the predetermined mass retained because the optimization results need to be redesigned by considering the production process to be carried out. Compared with other studies on different structural applications, topology optimization results applied to

the frame fuselage component of the MALE UAV successfully reduced an average of 26% of the overall frame weight [19].

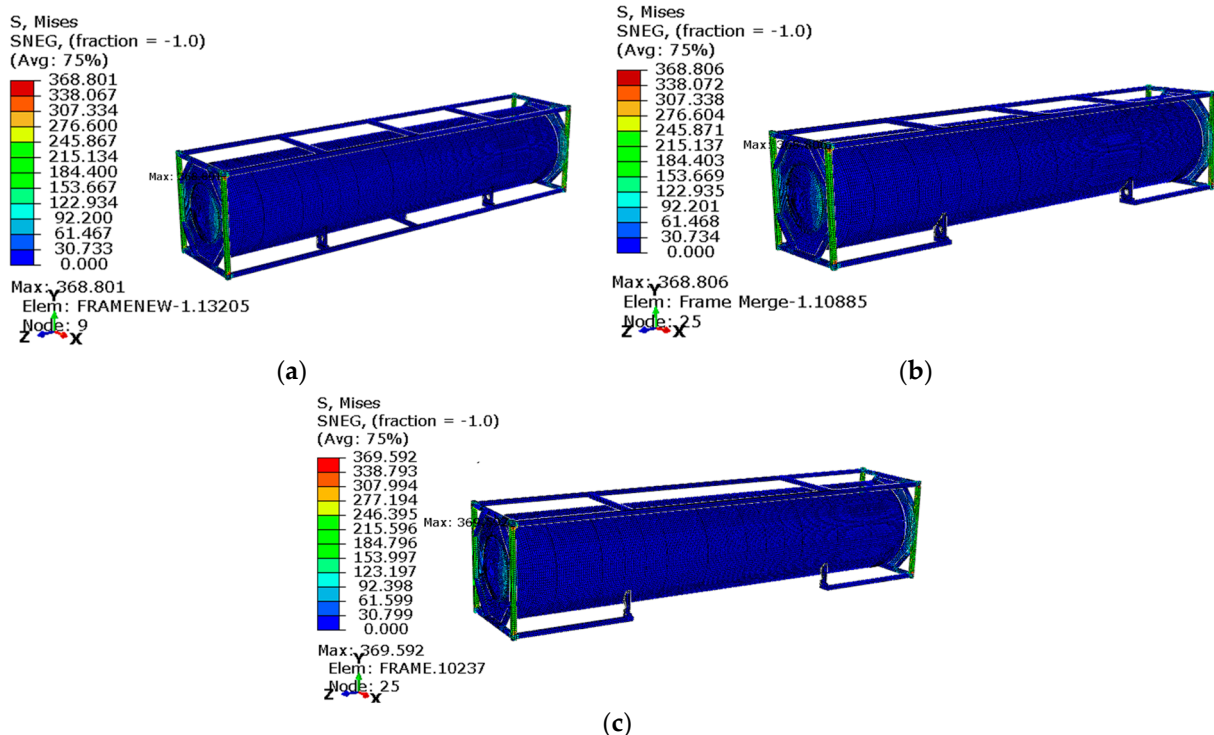


Figure 19. Stress contour of the optimized model in stacking load scenario: (a) 80% mass retained, (b) 70% mass retained, and (c) 60% mass retained.

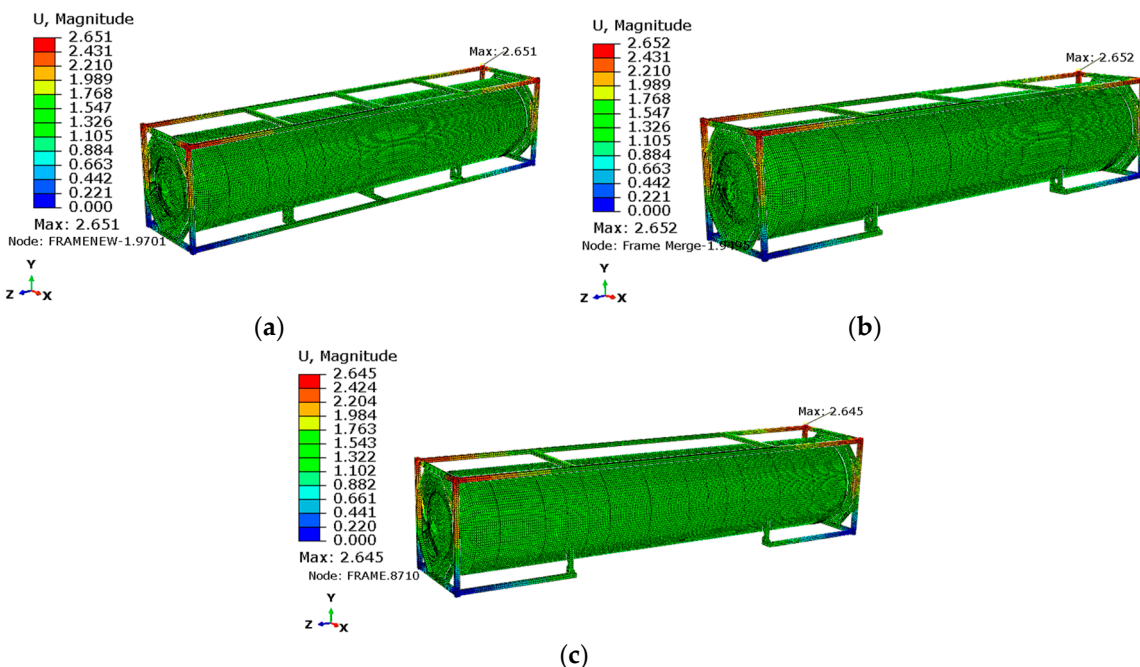


Figure 20. Displacement contour of the optimized model in stacking load scenario: (a) 80% mass retained, (b) 70% mass retained, and (c) 60% mass retained.

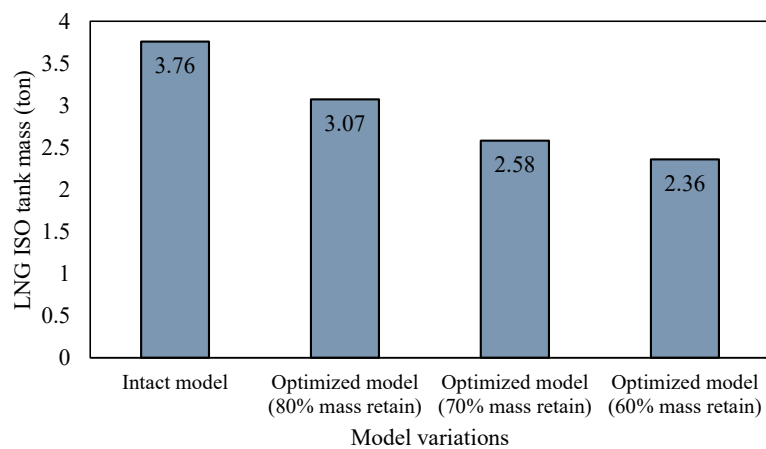


Figure 21. Comparison of mass between intact model and redesigned models.

3.4. Structural Performance by Increasing Thickness of Vertical Frame

In the previous analysis, the stress of the redesigned model of the structural frame in the stacking load scenario still exceeded the allowable stress value of the material, so modification of the redesigned frame model was required. For this loading, the vertical part of the structural frame was the most critical region with higher stress that needed to be considered, as seen in Figure 22. So, the increasing thickness of the vertical frame was evaluated by using three thickness variations of 11 mm, 12 mm, and 13 mm. It can be evaluated that the additional thickness of 1 mm increased the mass of the structural frame by 30 kg.

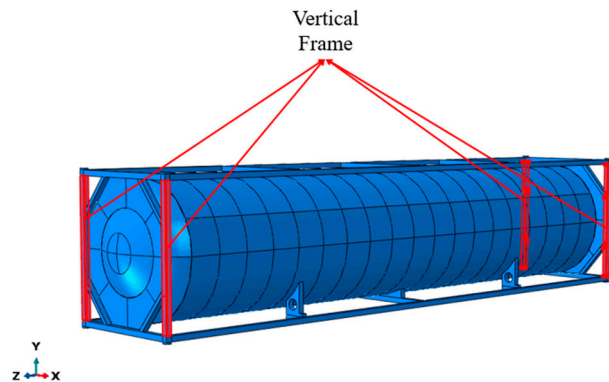


Figure 22. Additional thickness of the vertical frame of 40 ft ISO LNG tank.

A comparison of the simulation results of the stacking load scenario for the model with the increase in the vertical frame thickness is shown in Table 5. The increasing vertical frame thickness caused stress and displacement to decrease significantly in the structural frame, as seen in Figure 23. However, the stress experienced in the pressure vessel and corner casting remained the same. The percentage of stress reduction for the ISO corner casting and pressure vessels was only below 0.1%. It can be analyzed that with the increase of 1 mm thickness in the vertical frame due to stacking load, the structural frame still had a higher stress value near the allowable stress, especially in the 60 and 70% mass retained model. Moreover, a 12 mm vertical frame thickness due to stacking load caused a significant stress decrease in the 13.9–14.8% range. In addition, the vertical frame with 13 mm thickness had the highest stress reduction in the range of 20.5–22.4%. The optimum design was selected considering the maximum stress value, safety factor, and mass reduction. The frame design with a 12 mm vertical frame thickness had an optimum design with experienced stress below the allowable stress in all evaluated loads.

Table 5. Comparison of model simulation results with added thickness in stacking load scenario.

Vertical Frame Thickness (mm)	Mass Retained (%)	Frame Mass (Ton)	Structural Frame					
			Stacking Load		Lifting Load		Racking Load	
			Stress (MPa)	Displacement (mm)	Stress (MPa)	Displacement (mm)	Stress (MPa)	Displacement (mm)
10	80	3.07	368.80	2.58	61.86	0.43	75.66	0.98
	70	2.58	368.81	2.58	60.69	0.42	75.67	0.98
	60	2.36	369.59	2.57	60.42	0.42	76.16	0.96
	80	3.1	339.23	2.38	56.90	0.4	70.46	0.93
11	70	2.61	339.30	2.39	55.83	0.39	71.57	0.94
	60	2.39	340.08	2.38	55.60	0.39	70.20	0.91
	80	3.13	314.29	2.22	52.72	0.37	66.08	0.89
12	70	2.64	317.27	2.24	52.21	0.37	67.60	0.90
	60	2.42	315.07	2.22	51.51	0.36	68.82	0.87
	80	3.16	292.85	2.09	49.12	0.35	62.33	0.86
13	70	2.67	299.11	2.11	49.22	0.35	64.12	0.86
	60	2.45	293.56	2.08	47.99	0.34	67.18	0.84

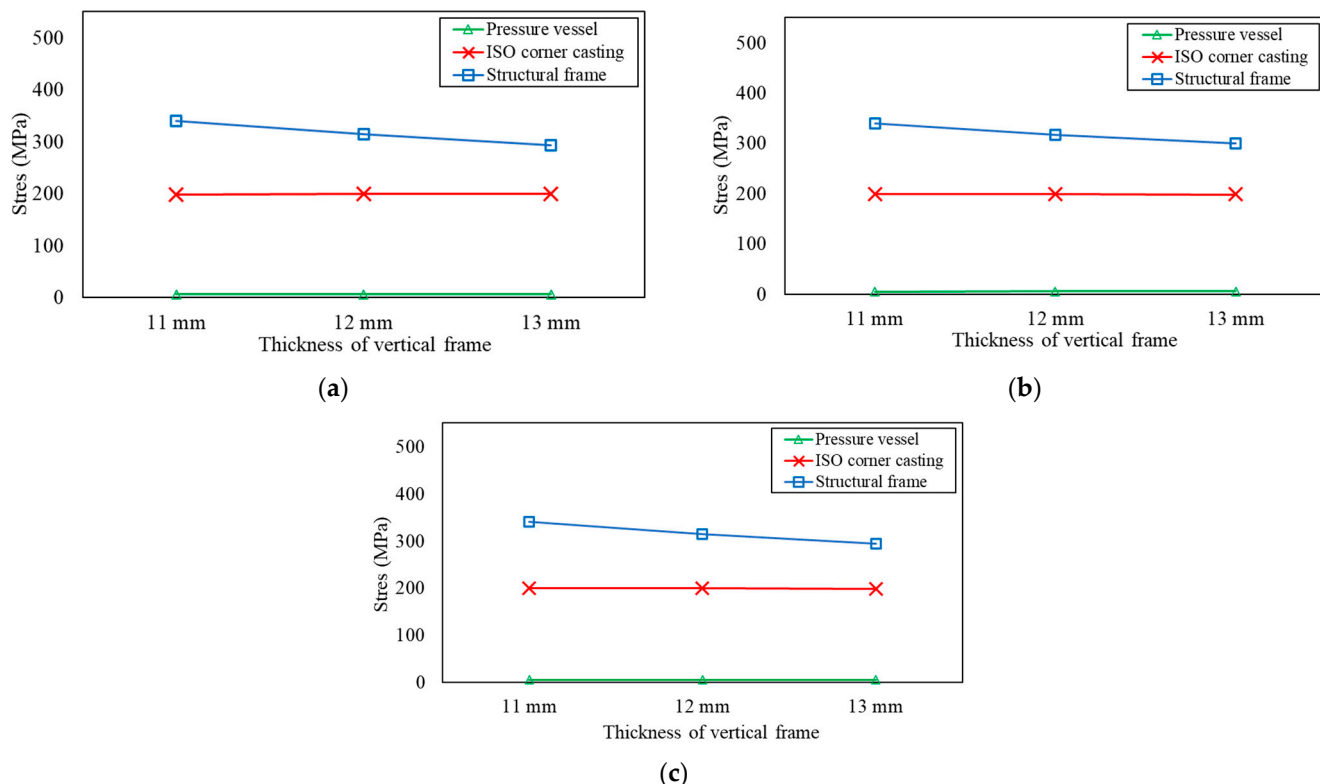
**Figure 23.** Comparison of maximum stress values in the modified redesigned models due to adding thickness to the vertical frame: (a) 80% mass retained, (b) 70% mass retained, and (c) 60% mass retained.

Figure 24 compares the displacement values for different vertical frame thicknesses under the stacking load scenario. In general, increasing the frame thickness reduces displacement values significantly in all three regions. The structural frame exhibits the highest percentage of displacement reduction, ranging from 5.8 to 7.4%. The percentage of displacement reduction in the pressure vessel and ISO corner casting sections was 5.7–7.2% and 5.2–6.9%, respectively.

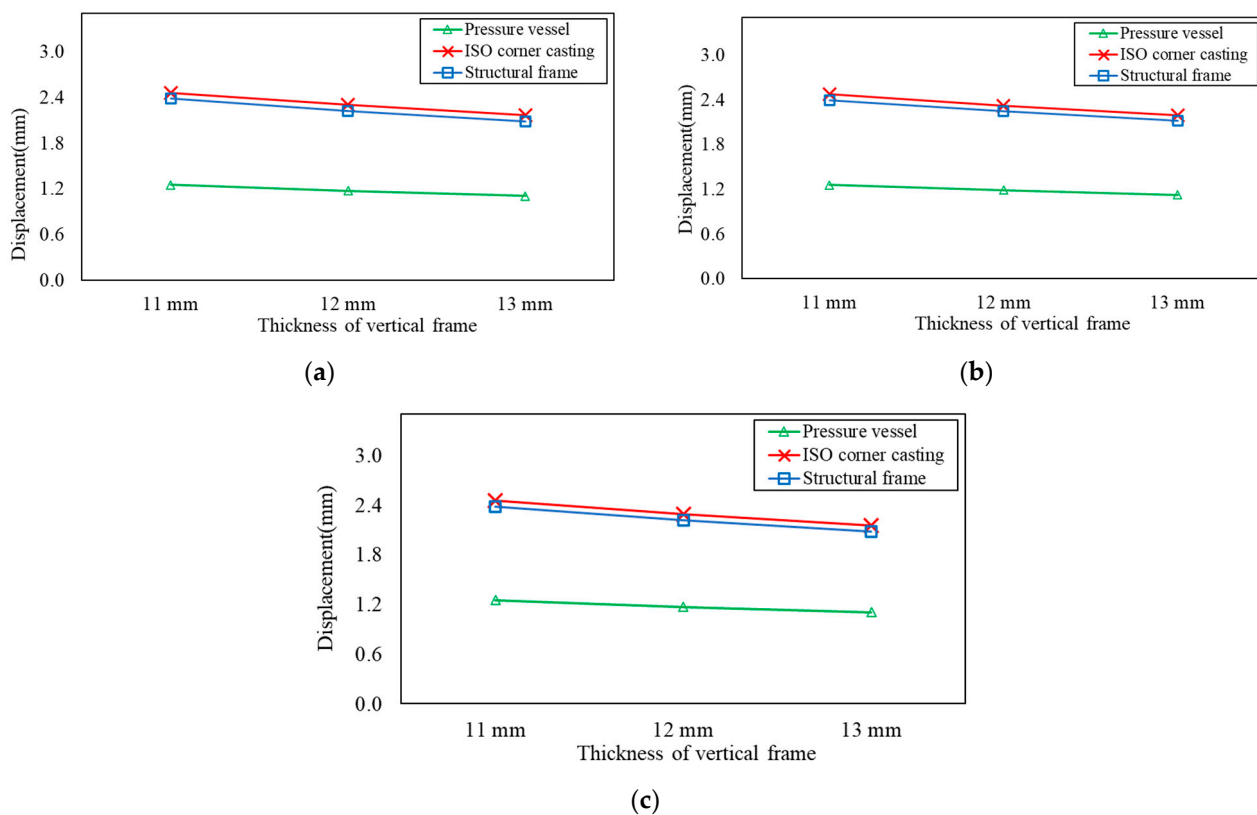


Figure 24. Comparison of maximum displacement values in the modified redesigned models due to adding thickness to the vertical frame: (a) 80% mass retained, (b) 70% mass retained, and (c) 60% mass retained.

The comparison of the safety factor of each mass retained is shown in Figure 25. It can be seen that the increasing vertical frame thickness can increase the safety factor value. It can be found that increasing vertical frame thickness to 12 and 13 mm successfully increases the safety factor of the structural frame due to the stacking load. Moreover, the comparison of the total mass due to increasing frame thickness is shown in Figure 26. It can be found that increasing the vertical frame thickness causes an increase in total mass of about 0.97–2.97%. It is a promising result because increasing thickness by about 1–3 mm can decrease the stress in the structural frame in the range of 8.01–22.4%. A previous study also mentioned that increasing the frame thickness of the LNG ISO tank is a better option than adding saddle supports. Increased frame thickness significantly decreases stress and displacement, surpassing the benefits of saddle supports [29]. In addition, integrating topology and shape optimization can reduce the weight of riverine patrol vessels by up to 4.21% [30].

Engineers may use topology optimization techniques to create structural designs that are not only lighter but also more material efficient. These improved designs may be used as models for other types of building projects, resulting in the creation of more sustainable and cost-effective structures across the construction industry. Topology optimization can assist in discovering potential defects and stress concentrations in structural designs, resulting in safer construction methods. This can lead to increased safety standards throughout the construction sector, lowering the potential of structural collapses and accidents on construction sites. Furthermore, this technology enables the development of more efficient structural designs, which can result in shorter construction durations and lower labor costs. By optimizing the construction process, businesses may execute projects more quickly and effectively, thus increasing industry production and profitability.

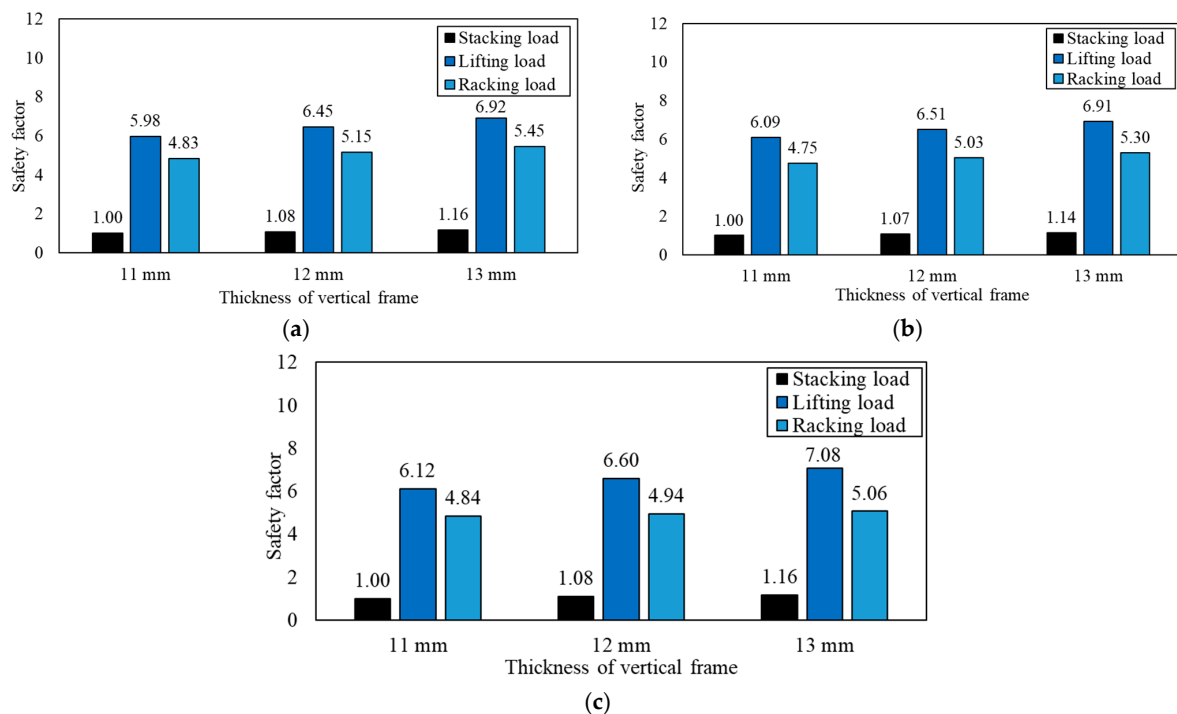


Figure 25. Comparison of safety factor on modified redesigned models due to adding thickness on the vertical frame: (a) 80% mass retained, (b) 70% mass retained, (c) 60% mass retained.

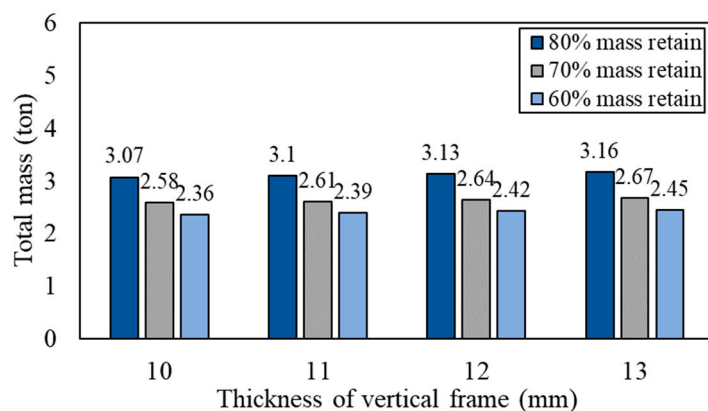


Figure 26. Mass comparison of modified redesigned models due to adding thickness to the vertical frame.

4. Conclusions

A series of topology optimization studies were conducted by ABAQUS/Standard to determine the most efficient LNG ISO tank frame design in terms of structural and weight aspects. In this case, mass retained was selected as the objective function to be minimized in the 60–80% range analyzed in three operational loading scenarios based on the ISO 1496 standard.

The results obtained show that the decreasing mass retained causes a stress increase, especially in the structural frame and ISO corner castings. The topology optimization result shows that the structural frame is the critical location that experiences the highest stress increase due to critical stacking load in the range from 18.09 to 18.35%. However, a promising result from the optimization process achieves weight savings of about 18.4–37.3%.

It can be found that several structural parts of the frame design, especially in the bottom part, including the longitudinal frame, transverse frame, and saddle support, experienced lower stress values and were suggested to be optimized. In contrast, the

vertical frame is a critical part that needs to be strengthened. Based on advanced FEA simulation, the increasing thickness of the vertical frame of about 1–3 mm can increase the total mass by about 0.97–2.97% and decrease the stress in the range of 8.01–22.4%. This is particularly crucial for LNG ISO containers as reducing weight can lead to lower transportation costs and increased payload capacity, thereby improving efficiency and reducing carbon emissions associated with transportation.

Author Contributions: Conceptualization, T.T., T.M. and R.H.; methodology, T.T., D.P.S. and W.A.; software, T.T. and M.A.; validation, M.A. and M.R.U.; formal analysis, T.M., A.B. and Y.Y.; writing—original draft preparation, T.T., T.M. and M.A.; writing—review and editing, D.P.S. and M.S.; visualization, T.M. and T.T.; supervision, D.P.S., R.H. and A.B.; project administration, M.R.U., A.B., M.S. and Y.Y.; funding acquisition, T.T., T.M. and D.P.S. All authors have read and agreed to the published version of the manuscript.

Funding: The authors extend their gratitude to the RISPRO-LPDP Ministry of Finance of the Republic of Indonesia for financing this study under the Research and Innovation for Advanced Indonesia (RIIM) batch 3 initiative, with contract number B-839/II.7.5/FR.06/5/2023.

Data Availability Statement: Data are contained within the article.

Acknowledgments: The authors would like to express their gratitude to the Laboratory of Ship Structure, Universitas Diponegoro, Semarang, Indonesia, for providing research facilities and assistance with the numerical tests.

Conflicts of Interest: The authors declare no conflicts of interest.

References

- Purwanto, W.W.; Muhamar, Y.; Pratama, Y.W.; Hartono, D.; Soedirman, H.; Anindhito, R. Status and outlook of natural gas industry development in Indonesia. *J. Nat. Gas Sci. Eng.* **2016**, *29*, 55–65. [[CrossRef](#)]
- Wahyuddin, W. Design of Blowdown Line LNG Filling Station ISO Tank. *J. Vocat. Stud. Appl. Res.* **2019**, *1*, 11–16. [[CrossRef](#)]
- Lee, D.Y.; Jo, J.S.; Nyongesa, A.J.; Lee, W.J. Fatigue Analysis of a 40 ft LNG ISO Tank Container. *Materials* **2023**, *16*, 428. [[CrossRef](#)]
- ASME. *ASME Boiler and Pressure Vessel Code Section VIII Division 1*; ASME: New York, NY, USA, 2019.
- Muttaqie, T.; Sasmito, C.; Iskendar; Kadir, A. Structural Strength Assessment of 20-ft LNG ISO Tank: An Investigation of Finite Element Analysis and ASME Design Guidance. *IOP Conf. Ser. Earth Environ. Sci.* **2022**, *972*, 012015. [[CrossRef](#)]
- Bhattacharyya, R.; Hazra, A. A study on stress analysis of ISO tank container. In Proceedings of the 58th Congress of the Indian Society of Theoretical and Applied Mechanics, Kolkata, India, 18–21 December 2013.
- Kim, T.W.; Kim, S.K.; Park, S.B.; Lee, J.M. Design of independent type-B LNG fuel tank: Comparative study between finite element analysis and international guidance. *Adv. Mater. Sci. Eng.* **2018**, *2018*, 5734172. [[CrossRef](#)]
- Wang, B.; Shin, Y.S.; Wang, X. Structural integrity assessment of independent type ‘C’ LNG carriers. In Proceedings of the 33rd International Conference on Ocean, Offshore and Arctic Engineering, San Francisco, CA, USA, 8–13 June 2014. [[CrossRef](#)]
- Pei, Y.Q.; Lu, S.; Liu, W.H. Structural design and research of type-C independent tank on small scale LNG ship. *J. Ship Prod. Des.* **2012**, *2*, 28–34.
- Watanabe, M.; Takada, R.; Okafuji, T.; Tsujii, H.; Kashiwagi, M.; Kamitani, Y. Structural design and construction method for “apple-shaped liquefied natural gas cargo tank” for LNG carriers. *Mitsubishi Heavy Ind. Tech. Rev.* **2016**, *53*, 11–18.
- Wang, Z.; Qian, C. Strength analysis of LNG tank container for trains under inertial force. *J. Phys. Conf. Ser.* **2020**, *1549*, 032107. [[CrossRef](#)]
- Zhaochun, R.; Ying, L.; Chao, H. Stress analysis of LNG tank container. *Ref. Chem. Ind.* **2018**, *29*, 42–43.
- Paul, P.R.; Chowdary, V.L. Design and Static Analysis of Different Pressure Vessels and Materials Using FEM Method. *Int. J. Sci. Res. Eng. Trends* **2020**, *5*, 93–99.
- Islam, M.S.; Paul, S.C. Topology Optimization of an Oiltanker Bulkhead Subjected to Hydrostatic Loads. *J. Nav. Archit. Mar. Eng.* **2021**, *18*, 207–215. [[CrossRef](#)]
- Wang, Q.; Chu, G.; Li, S.; Renjie, L. Research on Topology optimization Method for Tanker Structures in Cargo Tank Region. In Proceedings of the TSCF 2016 Shipbuilders Meeting, Busan, Republic of Korea, 26–27 October 2016; pp. 1–18.
- Zhang, C.; Zeng, Z.; Ji, C. Structure design of the ship pedestal based on topology optimization. In Proceedings of the VIII International Conference on Computational Methods in Marine Engineering, Göteborg, Sweden, 13–15 May 2019; pp. 754–770.
- Kendibilir, A.; Motlagh, P.L.; Kefal, A. Three-Dimensional Topology Optimization for Marine Structure Components Using Non-Local Methods. In Proceedings of the 34th Asian-Pacific Technical Exchange and Advisory Meeting on Marine Structures (TEAM 2020/21), Istanbul, Turkey, 6–8 December 2021.
- Pingale, H.; Patel, N. Topology Optimization and Manufacturing Aspects. In Proceedings of the IRAJ International Conference, Pune, India, 15 April 2018; Volume 6, pp. 65–68.

19. Aribowo, A.; Adhynugraha, M.; Megawanto, F.; Hidayat, A.; Muttaqie, T.; Wandono, F.; Nurrohmad, A.; Chairunnisa; Saraswati, S.; Wiranto, I.; et al. Finite element method on topology optimization applied to laminate composite of fuselage structure. *Curved Layer. Struct.* **2023**, *10*, 20220191. [[CrossRef](#)]
20. Kim, H.S.; Kim, H.S.; Park, B.; Lee, K. 3D Topology Optimization of Fixed Offshore Structure and Experimental Validation. *J. Ocean Eng. Technol.* **2020**, *34*, 263–271. [[CrossRef](#)]
21. Deng, W.; Tian, X.; Han, X.; Liu, G.; Xie, Y.; Li, Z. Topology optimization of jack-up offshore platform leg structure. *Proc. Inst. Mech. Eng. Part M J. Eng. Marit. Environ.* **2021**, *235*, 165–175. [[CrossRef](#)]
22. Nugroho, A.C.P.T.; Sunaryo; Noor, F.M. A Technical Study of Vessel Fleet Requirements for LNG Logistic Systems using ISO Tank Container in the Maluku Region. *Wave J. Ilm. Teknol. Marit.* **2020**, *14*, 33–42.
23. ISO 1496-3:2019-4; Series 1 Freight Containers-Specification and Testing—Part 3: Tank Containers for Liquids Gases and Pressurized Dry Bulk. ISO: Geneva, Switzerland, 2019.
24. ASME. *ASME Boiler and Pressure Vessel Code Section II Part D Properties*; ASME: New York, NY, USA, 2019.
25. Mansour, W.; Li, W.; Wang, P.; Badawi, M. Experimental and numerical evaluations of the shear performance of recycled aggregate RC beams strengthened using CFRP sheets. *Eng. Struct.* **2024**, *301*, 117368. [[CrossRef](#)]
26. Giriunas, K.; Sezen, H.; Dupax, R. Evaluation, modeling, and analysis of shipping container building structures. *Eng. Struct.* **2012**, *43*, 48–57. [[CrossRef](#)]
27. Fahy, M.; Tiernan, S. Finite element analysis of ISO tank containers. *J. Mater. Process. Technol.* **2001**, *119*, 293–298. [[CrossRef](#)]
28. Prabowo, A.R.; Laksono, F.B.; Sohn, J.M. Investigation of structural performance subjected to impact loading using finite element approach: Case of ship-container collision. *Curved Layer. Struct.* **2020**, *7*, 17–28. [[CrossRef](#)]
29. Purnamasari, D.; Tuswan, T.; Muttaqie, T.; Sandjaja, I.; Machfudin, A.; Rizal, N.; Rahadi, S.; Sasmito, A.; Zakki, A.F.; Mursid, O. Structural assessment of 40 ft mini LNG ISO tank: Effect of structural frame design on the strength performance. *Curved Layer. Struct.* **2024**, *11*, 20220219. [[CrossRef](#)]
30. Algarra, G.A.M.; Tovar, A. Integrating topology and shape optimization: A way to reduce weight in structural ship design. *Ship Sci. Technol.* **2009**, *3*, 83–92.

Disclaimer/Publisher's Note: The statements, opinions and data contained in all publications are solely those of the individual author(s) and contributor(s) and not of MDPI and/or the editor(s). MDPI and/or the editor(s) disclaim responsibility for any injury to people or property resulting from any ideas, methods, instructions or products referred to in the content.